JOURNAL OF
ENVIRONMENTAL
SCIENCES

ELSEVIER

Science Press

JOURNAL OF ENVIRONMENTAL SCIENCES

(http://www.jesc.ac.cn)

Submission declaration

Submission of an article implies that the work described has not been published previously (except in the form of an abstract or as part of a published lecture or academic thesis), that it is not under consideration for publication elsewhere. The submission should be approved by all authors and tacitly or explicitly by the responsible authorities where the work was carried out. If the manuscript accepted, it will not be published elsewhere in the same form, in English or in any other language, including electronically without the written consent of the copyright-holder.

Submission declaration

Submission of the work described has not been published previously (except in the form of an abstract or as part of a published lecture or academic thesis), that it is not under consideration for publication elsewhere. The publication should be approved by all authors and tacitly or explicitly by the responsible authorities where the work was carried out. If the manuscript accepted, it will not be published elsewhere in the same form, in English or in any other language, including electronically without the written consent of the copyright-holder.

CONTENTS

Rapid decolorization of Acid Orange II aqueous solution by amorphous zero-valent iron

Changqin Zhang[1,2], Zhengwang Zhu[1], Haifeng Zhang[1,*], Zhuangqi Hu[1]

1. Shenyang National Laboratory for Materials Science, Institute of Metal Research, Chinese Academy of Sciences, Shenyang 110016, China
2. Graduate School of Chinese Academy of Sciences, Beijing 100039, China

Abstract

Some problems including low treatment capacity, agglomeration and clogging phenomena, and short working life, limit the application of pre-treatment methods involving zero-valent iron (ZVI). In this article, ZVI was frozen in an amorphous state through a melt-spinning technique, and the decolorization effect of amorphous ZVI on Acid Orange II solution was investigated under varied conditions of experimental variables such as reaction temperature, ribbon dosage, and initial pH. Batch experiments suggested that the decolorization rate was enhanced with the increase of reaction temperature and ribbon dosage, but decreased with increasing initial solution pH. Kinetic analyses indicated that the decolorization process followed a first order exponential kinetic model, and the surface-normalized decolorization rate could reach 2.09 L/(m^2·min) at room temperature, which was about ten times larger than any previously reported under similar conditions. Recycling experiments also proved that the ribbons could be reused at least four times without obvious decay of decolorization rate and efficiency. This study suggests a tremendous application potential for amorphous ZVI in remediation of groundwater or wastewater contaminated with azo dyes.

Key words: amorphous zero-valent iron; Acid Orange II; decolorization; surface-normalized decolorization rate; recycle

DOI: 10.1016/S1001-0742(11)60894-2

Introduction

Residual dyes from effluents of the textile dyeing and finishing industry have attracted major environmental attention because of their widespread contamination of water and soil, owing to their high toxicity and poor degradability (Zhao et al., 2010; Qu et al., 2008). Within the overall category of synthetic textile dyestuffs, azo dyes constitute about half of global production, and during dyeing operation processes, about 15% end up in wastewaters (Park and Choi, 2003). Azo dyes usually have complex aromatic structures that are highly resistant to microorganisms and recalcitrant to conventional biological wastewater treatment processes (Pagga and Brown, 1986; Shu et al., 1994; Manu and Chaudhari, 2003), and constitute a significant burden on the environment. Traditional physical methods such as flocculation and adsorption simply transfer the pollutants to another phase rather than destroying them (Dutta et al., 2001); some chemical treatment technologies such as UV/H$_2$O$_2$, UV/O$_3$, UV/TiO$_2$ and the Fenton reaction have served to remove color and achieve final mineralization effectively, yet are limited to the laboratory because of their rigorous operation conditions (Ruppert et al., 1994; Shu and Huang, 1995; Ozer and Ferry, 2001; Muruganandham and Swaminathan, 2004; Chen and Zhu, 2007).

During past decades, zero-valent iron (ZVI) has shown the greatest promise for the reduction of many common environmental contaminants (Gillham and O'Hannesin, 1994; Agrawal and Tratnyek, 1996; Roberts et al., 1996; Orth and Gillham, 1996; Cao et al., 1999; Kao et al., 2001; Lai et al., 2007), and innovative methods such as nanotechnology using nanoscale ZVI (NZVI) particles have been developed for application in environmental treatment and remediation (Masciangioli and Zhang, 2003). A few investigations have reported dye wastewater treatment by ZVI particles. Efficient decolorization by ZVI particles was demonstrated for five azo dyes under anaerobic conditions via cleavage of the azo link cleavage of the dye molecules (Cao et al., 1999), and an innovative method using NZVI particles to increase the specific surface area of ZVI has also been developed for the decolorization of azo dyes (Masciangioli and Zhang, 2003; Shu et al., 2007; Fan et al., 2009). The advantages of ZVI particles for dye color removal include ease in use as a pre-treatment process, easy recycling of the spent iron powder removal with magnets as well as low residual iron concentration and no necessity for further treatment of the effluents (Chang et al., 2006). In this study, by virtue of a melt-spinning technique, crystalline ZVI was successfully frozen into the amorphous state in Fe-Si-B amorphous ribbons. In the ribbons, the amorphous ZVI was expected to have different

---

performance from its crystalline counterpart in the degradation of azo dyes. Using melt-spun Fe-Si-B amorphous ribbons, a feasibility study of the use of amorphous ZVI for removing the color and organic constituents of an azo dye (Acid Orange II) solution was proposed through study of the effects of experimental variables such as temperature, ribbon dosage, and initial solution pH. Additionally, the recycling of the ribbons and reaction kinetics for the decolorization process were also investigated.

1 Materials and methods

1.1 Preparation and characterization of Fe-Si-B amorphous ribbons

An alloy ingot with nominal composition of $Fe_{78}Si_8B_{14}$ alloy was produced by arc melting a mixture of Fe, Si and Fe-B alloy under a Ti-gettered Ar atmosphere. The purity of Fe and Si was higher than 99.9%, and Fe-B alloy with a purity of 99% was purchased from Liaoyang International Boron Alloys Co., China. The ingot was then remelted in a quartz tube by induction melting, followed by roller spinning to make ZVI frozen into ribbons. The amorphous ribbons were about 2 mm wide, 30–40 μm thick and up to several meters long.

The structure of the ribbons was examined by X-ray Diffraction (XRD) with Cu-$K\alpha$ radiation (D/max-2500PC, Rigaku Co., Japan), and transmission electron microscopy (TEM) (Tecnai G2 20, FEI Co., USA) and a scanning electron microscope (SEM) (S360, Cambridge Instrument, UK) was used to observe the surface morphology of the ribbons.

1.2 Decolorization procedures

The ribbons were cut into pieces of 2×10 mm^2 for subsequent decolorization procedures. Acid Orange II powder ($\geqslant$ 99.9 wt.%, purchased from Tianjin Yuhua Co., China) was dissolved in distilled water to obtain an aqueous solution. After being cut, the ribbons were cleaned with distilled water, and then rinsed with ethanol ($\geqslant$ 99.9 wt/%) twice. A 180-mL solution of 100 mg/L dye and amorphous ribbons were added to a beaker; in all experiments where ribbon dosage was not a variable, the nominal surface area of the ribbons was 15,000 mm^2 to ensure a constant iron surface area concentration of 8.33×10^{-2} m^2/L. Repeated decolorization experiments were carried out to investigate the feasibility of recycling the glassy ribbons in solutions containing 200 mg/L dye and 15,000 mm^2 amorphous ribbons. The beaker was placed in a constant temperature water–bath trough at controlled temperatures, and mechanical agitation of 200 r/min was applied in the beaker during the reaction process. About 4 mL solution was taken from the beaker at intervals, and subjected to UV-Vis spectrum scanning from 200 to 600 nm using a UV-Visible spectrophotometer (Model V-550 JAS. Co., USA) after being filtered through a 0.45 μm membrane filter.

The dye concentration of the solution can be calculated from the ratio of the intensity of the absorbance peak in the visible region at λ_{max} to that of the reference solution by the following equation:

$$C_t = C_0 \times \lambda_{max\ t}/\lambda_{max\ 0} \tag{1}$$

where, C_0 (mg/L) and C_t (mg/L) are the dye concentrations at time 0 and t, and $\lambda_{max\ 0}$ (a.u.) and $\lambda_{max\ t}$ (a.u.) are the intensities of the absorbance peak in the visible region of the solution at time 0 and t, respectively.

2 Results and discussion

2.1 Characterization of the ribbon

The XRD pattern and TEM diffraction image of the ribbons obtained by the melt-spinning technique are presented in Fig. 1a. The amorphous nature of the ribbon can be verified by the broad peak in the XRD pattern and the single dispersive halo in the TEM diffraction image. These results demonstrate that the structure of the ribbon is a short-range ordered and long-range disordered structure, and the ZVI is in an amorphous state.

Figure 1b shows the SEM images of both the free surface and the surface in contact with the roller during fabrication of the ribbon. It can be seen that the free surface is nearly perfectly smooth, and the roll-contact surface is relatively rough. Based on the SEM image, it is reasonable to deduce that the area increment relative to the nominal area due to roughness is not very significant.
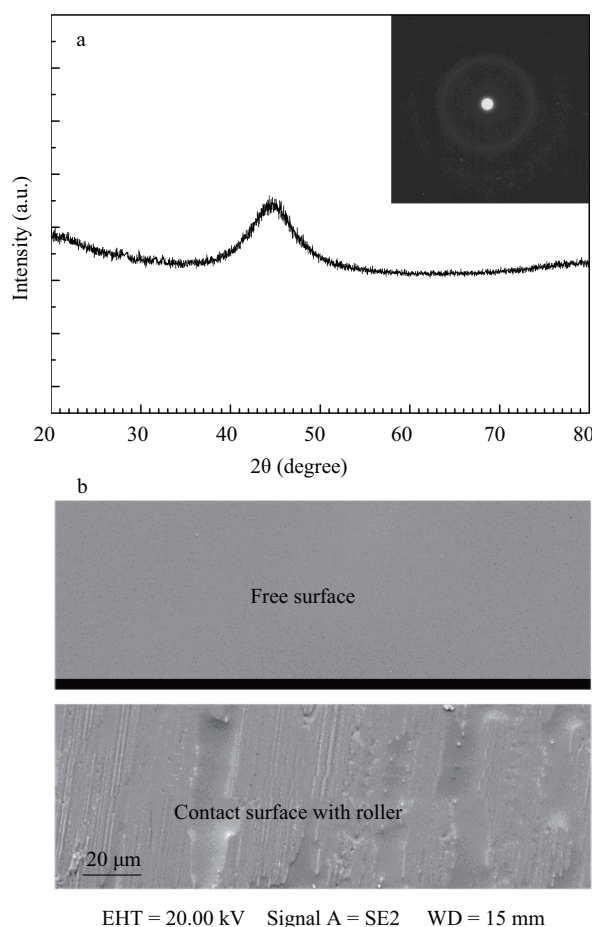

Fig. 1 XRD pattern, TEM diffraction image (a) and SEM image (b) of the $Fe_{78}Si_8B_{14}$ ribbons obtained by melt-spining technique.

2.2 Effect of decolorization temperature

The UV-Vis spectrum changes as a function of reaction time at 40°C are illustrated in Fig. 2. The strong absorbance peak at λ_{max} = 484 nm in the visible region originates from a conjugated structure formed by the azo bonds, the intensity of which denotes the dye concentration in the solution (Cao et al., 1999; Nam and Tratnyek, 2000). The other two bands at 230 and 310 nm in the ultraviolet region are ascribed to the benzene and naphthalene rings of the dye, respectively. The bands at λ_{max} become weaker with time, which reveals the cleavage of the azo bonds and the decomposition of Acid Orange II in the solution. Along with the cleavage of the azo bonds, -NH$_2$ groups are also formed, which can be verified by the increasing intensity of the absorbance peak at 246 nm as shown in Fig. 2 (Zhang et al., 2011).

Through nonlinear curve fitting, it is deduced that the degradation process fits very well with first order exponential decay kinetics as proposed by Cao et al. (1999) and Nam and Tratnyek (2000) as follows:

$$C_t/C_0 = \exp(-kt) \tag{2}$$

where, k (min^{-1}) is the observed rate constant, and t (min) is the reaction time.
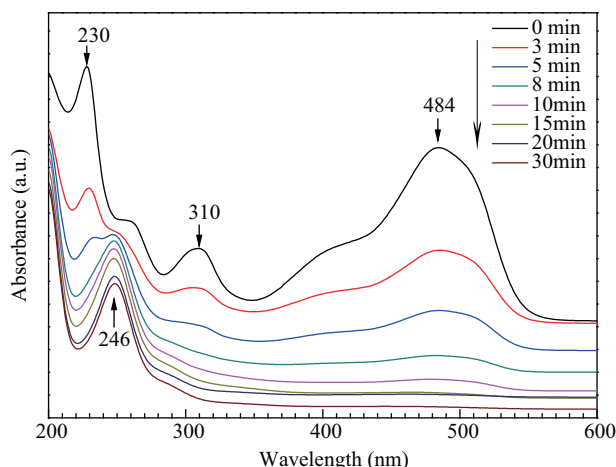

Fig. 2 UV-Vis spectrum change as a function of reaction time. Initial Acid Orange II concentration 100 mg/L; ribbon dosage 0.0833 m^2/L; initial pH 6; temperature 40°C.

Experiments were carried out in the temperature range of 25–50°C to study the effect of temperature on the decolorization of Acid Orange II, and the decolorization rate constants could be obtained by nonlinear regression. The values along with surface-area-normalized rate constants are listed in Table 1.

Based on the obtained kinetic rate constants at different temperatures, the activation energy (E_a, kJ/mol) of the decolorization process of Acid Orange II by amorphous ZVI can be obtained according to the Arrhenius equation:

$$\ln k = -E_a/RT + \ln A \tag{3}$$

It is calculated that E_a is 27.9 kJ/mol for the decolorization process of Acid Orange II by the amorphous ZVI over the temperature range of 25–50°C (Zhang et al., 2011). The temperature effect is important in providing some insight into the reaction mechanism (Liou et al., 2005; Fan et al., 2009). For ordinary thermal reactions, the activation energy is usually between 60 and 250 kJ/mol (Chen and Zhu, 2007); for the reaction of NZVI decolorizing azo dyes, the activation energy is 35.9 kJ/mol (Fan et al., 2009). Our results imply that the decolorization of Acid Orange II by amorphous ZVI requires a relatively low energy, which may also help us to understand the reason why amorphous ZVI has a much larger surface-normalized decolorization rate (k_{SA}) than crystalline ZVI as aforementioned.

2.3 Effect of the ribbon dosage

It is well known that the degradation reaction of organic compounds using ZVI occurs on the surface of iron metal, and it is the same for azo dyes (Weber, 1996). When effective collision between dye molecules and ribbons takes place, amorphous ZVI in the ribbons loses electrons while the dye molecule accepts electrons, combines with H$^+$ and turns into a transitional product. Thus, surface area should affect the degradation reaction. In this experiment, the decolorization of Acid Orange II with different ribbon dosages, 0.0833, 0.0556, and 0.0278 m^2/L, was studied. Figure 3a shows the reaction curves under different ribbon dosages. By nonlinear regression, the decolorization rate constants were obtained as presented in Table 1. Through linear regression, it is clear that, with increasing ribbon

Table 1 Results of nonlinear regression of experimental data

C_0 (mg/L)	Recycle time	Temperature (°C)	Ribbon dosage (m^2/L)	Initial pH	k (min^{-1})	k_{SA} (L/(m^2·min))	R^2
200	1	40	0.0833	6	0.252	3.03	0.99673
200	2	40	0.0833	6	0.249	2.99	0.99871
200	3	40	0.0833	6	0.281	3.37	0.99977
200	4	40	0.0833	6	0.295	3.54	0.99999
100	1	25	0.0833	6	0.174	2.09	0.99976
100	1	30	0.0833	6	0.205	2.46	0.99819
100	1	40	0.0833	6	0.299	3.59	0.99970
100	1	50	0.0833	6	0.412	4.95	0.99989
100	1	40	0.0556	6	0.201	3.60	0.99992
100	1	40	0.0278	6	0.087	3.13	0.99979
100	1	25	0.0833	3	0.443	5.32	0.99913
100	1	25	0.0833	1	0.214	2.57	0.99999
100	1	25	0.0833	11	–[a]	–	–

[a] Degradation process does not fit with first order exponential decay kinetics at this initial pH value (pH = 11), so the values of rate constant (k), surface-normalized decolorization rate (k_{SA}) and R^2 make no sense.
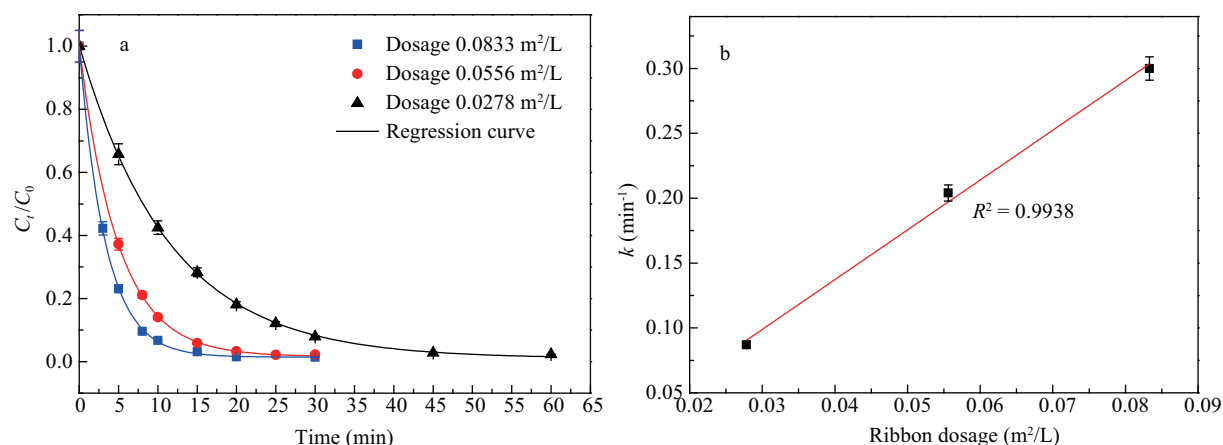
Fig. 3 Effect of ribbon dosage on the decolorization of Acid Orange II (a) and linear regression of decolorization rate constant (k) versus ribbon dosage (b). Initial Acid Orange II concentration 100 mg/L; initial pH 6; temperature 40°C.

dosage, the decolorization rate of Acid Orange II is increased. The reaction constant is linearly correlated with relative ribbon dosage as Fig. 3b shows and the reaction rate constant k equals 3.84 ribbon dosage according to our results.

2.4 Effect of initial pH

Solution pH has been considered as one of the important factors in ZVI-contaminant systems, therefore the effect of initial solution pH on the decolorization of Acid Orange II was studied, and the results are shown in Fig. 4. At acidic and circum-neutral initial pH, Acid Orange II solutions were almost completely decolorized within 30 min. As the initial pH increased to the alkaline pH range, the final decolorization efficiency decreased to a very low level in the same reaction time, and our results illustrated that the decolorization processes followed different kinetics. By nonlinear regression, it can be seen that the decolorization process under acidic and circum-neutral initial pH followed a first order kinetic model while the process under alkaline conditions followed a different model. Moreover, the decolorization mechanism was probably different. Compared with the UV-Vis spectra of Acid Orange II as a function of reaction time for acidic and circum-neutral

initial pH, in the UV-Vis spectra of Acid Orange II for alkaline pH, all peaks weaken synchronously as a function of reaction time, and no peaks at new positions appear as the inset of Fig. 4b shows. When the solution pH is in the alkaline pH range, the oxide surface becomes negatively charged. The ribbon surface could easily be covered by corrosion products under alkaline conditions, which may prevent sufficient collisions between ribbons and dye molecules, leading to a decay of the decolorization rate. It is reasonable to deduce that this process may be a physical adsorption dominant process, during which Acid Orange II cannot be degraded, and the addition of NaOH plays a key role in inhibiting the process.

In addition, as shown in Table 1, although HCl addition drives the decolorization process, the decolorization rate constant did not increase monotonically with HCl addition. The acid-driven effect can be ascribed to the fact that at lower pH, the surface of ribbons is positively charged (Li et al., 2006), and the dye molecules with a sulfonate group were negatively charged, which is favorable for the adsorption of dye onto the ribbon surface. But on the other hand, if too much acid was added, excessive H^+ would adsorb on the surface of the ribbons, gain electrons from the ribbons to form H_2 bubbles, occupy the reactive
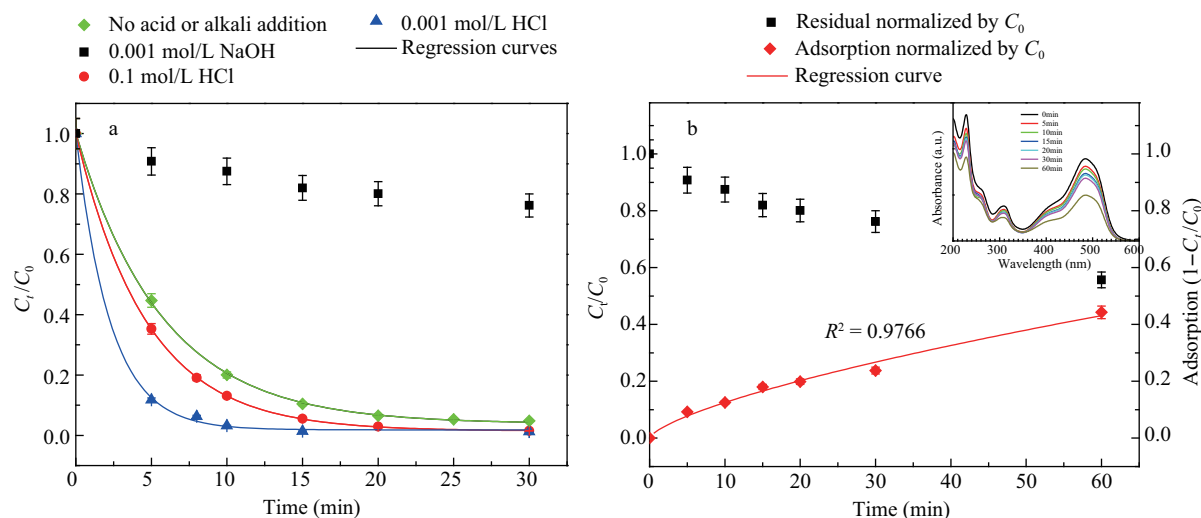

Fig. 4 Effect of acid and alkali addition (a) and 0.001 mol/L NaOH addition (b) on the decolorization of Acid Orange II. Inset: UV-Vis spectrum change as a function of reaction time. Initial Acid Orange II concentration 100 mg/L; ribbon dosage 0.0833 m²/L; temperature 25°C.

sites, and finally slow the decolorization rate. This result suggests that weak acidic and circum-neutral initial pH favor dye decolorization, while too strongly acidic initial pH may induce side effects to the decolorization process.

2.5 Recycling of the ribbons

To assess the feasibility of recycling the glassy ribbons, repeated decolorization experiments were done one after another with fresh solutions and the ribbons used in the previous cycle, and the results are shown in Fig. 5. It can be seen that after 30 min, the intensity of the absorbance peak at λ_{max} was nearly zero, and the decolorization efficiency decays little until the fourth cycle, which means the ribbons can be reused conveniently without any treatment. It is worthwhile to note that the decolorization rate constants (k) of the third and fourth cycles are 0.281 and 0.295 min^{-1} respectively, which are larger than those of the first and second cycles, as Table 1 presents. This phenomenon may be attributed to the increment of the surface area because of the desquamation of the ribbon during the decolorization process.

2.6 Decolorization reaction mechanism analysis

The decolorization effect of the ribbons is attributed to the ZVI being frozen in an amorphous state in the ribbons (Nam and Tratnyek, 2000; Saxe et al., 2006; Hou et al., 2007; Zhang et al., 2010). During the decolorization process, amorphous ZVI in the glassy ribbons with high activity can be released into the solution gradually, and directly reacts with dye molecules by the reaction of Fe–2e$^-$ = Fe^{2+}, leading to the decolorization of the dye solution. Moreover, the reaction between ZVI and H$_2$O or H$^+$ can generate abundant atomic [H], and this kind of [H] has high reactivity, which induces the cleavage of azo bonds (–N=N–), thus destroying the chromophore groups of the azo dye (Sohn et al., 2006; Zhang et al., 2010). Thus appropriate HCl addition can drive the decolorization process because of the generation of more atomic [H] and the adsorption effect as aforementioned.
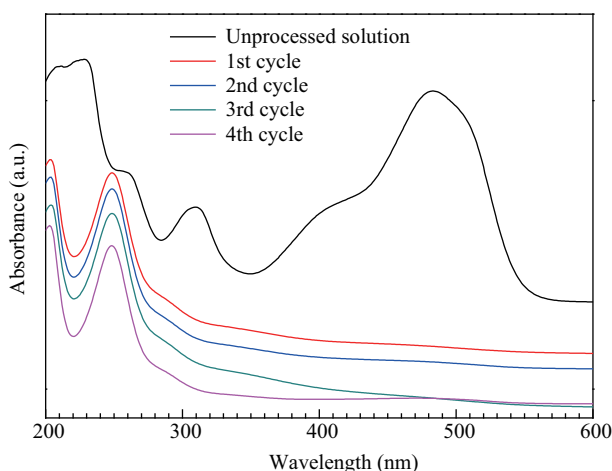

Fig. 5 UV-Vis spectra of Acid Orange II solutions reacting with amorphous ribbons for four 30 min cycles. Initial Acid Orange II concentration 200 mg/L; ribbon dosage 0.0833 m^2/L; initial pH 6; temperature 40°C. During every cycle, the solution concentration was 200 mg/L, and ribbons were the ribbons used during the previous cycle without any treatment.

Nam and Tratnyek (2000) also proposed the parameter, surface-normalized decolorization rate (k_{SA}), which equals to k divided by ribbon dosage, as the decolorization ability indicator of different materials. k_{SA} was considered to reflect the decolorization ability more essentially than k, because the parameter k_{SA} eliminates the effect of the surface area of decolorization materials. Compared with the results reported by Nam and Tratnyek (2000) that k_{SA} was approximately 0.268 L/(m^2·min) where ZVI in a micron scale was employed to decolorize Acid Orange II under similar conditions, the amorphous ZVI in the present study reduces the azo dyes much faster than micro-ZVI does, and k_{SA} can reach 2.09 L/(m^2·min), which is one order of magnitude larger than that of crystalline ZVI.

The temperature effect study on the decolorization of Acid Orange II by the amorphous ZVI reveals that this reaction requires a relatively lower energy than ordinary thermal reactions and the reaction of crystalline ZVI in decolorizing azo dyes, which means that this reaction occurs more easily under similar reaction conditions. Fe$_{78}$Si$_8$B$_{14}$ amorphous ribbons may play a role as a better catalyst for the reaction, and provide more reactive sites than crystalline ZVI owing to the thermodynamically higher energy state of the non-equilibrium structure.

3 Conclusions

In summary, this work provides a potential technique for the pre-treatment of difficultly degradable azo dye wastewater. Based on the discussion above, it can be concluded that the decolorization process of aqueous Acid Orange II solution by amorphous ZVI (Fe-Si-B amorphous ribbons) can be described by a first order kinetic model, and the surface-normalized decolorization rate can reach a value about ten times larger than any previously reported. Recycling experiments proved that the ribbons could be reused at least four times without obvious decay of the decolorization rate and efficiency. Increase in temperature was found to greatly accelerate the decolorization, and an appropriate dosage of amorphous ribbons and initial pH were important for the decolorization of Acid Orange II. Generally, a greater ribbon dosage could yield greater reaction rate and decolorization efficiency, while too strongly acidic initial pH caused side effects to the decolorization process, although weakly acidic and circum-neutral initial pH favored dye decolorization.

References

Agrawal A, Tratnyek P G, 1996. Reduction of nitro aromatic compounds by zero-valent iron metal. *Environmental Sci-*

ence & Technology, 30(1): 153–160.

Cao J S, Wei L P, Huang Q G, Wang L S, Han S K, 1999. Reducing degradation of azo dye by zero-valent iron in aqueous solution. *Chemosphere*, 38(3): 565–571.

Chang M C, Shu H Y, Yu H H, Sung Y C, 2006. Reductive decolourization and total organic carbon reduction of the diazo dye CI Acid Black 24 by zero-valent iron powder. *Journal of Chemical Technology and Biotechnology*, 81(7): 1259–1266.

Chen J X, Zhu L Z, 2007. Heterogeneous UV-Fenton catalytic degradation of dyestuff in water with hydroxyl-Fe pillared bentonite. *Catalysis Today*, 126(3-4): 463–470.

Dutta K, Mukhopadhyay S, Bhattacharjee S, Chaudhuri B, 2001. Chemical oxidation of methylene blue using a Fenton-like reaction. *Journal of Hazardous Materials*, 84(1): 57–71.

Fan J, Guo Y H, Wang J J, Fan M H, 2009. Rapid decolorization of azo dye methyl orange in aqueous solution by nanoscale zerovalent iron particles. *Journal of Hazardous Materials*, 166(2-3): 904–910.

Gillham R W, O'Hannesin S F, 1994. Enhanced degradation of halogenated aliphatics by zero-valent iron. *Ground Water*, 32(6): 958–967.

Hou M F, Li F B, Liu X M, Wang X G, Wan H F, 2007. The effect of substituent groups on the reductive degradation of azo dyes by zerovalent iron. *Journal of Hazardous Materials*, 145(1-2): 305–314.

Kao C M, Chou M S, Fang W L, Liu B W, Huang B R, 2001. Regulating colored textile wastewater by 3/31 wavelength admi methods in Taiwan. *Chemosphere*, 44(5): 1055–1063.

Lai P, Zhao H Z, Wang C, Ni J R, 2007. Advanced treatment of coking wastewater by coagulation and zero-valent iron processes. *Journal of Hazardous Materials*, 147(1-2): 232–239.

Li X Q, Elliott D W, Zhang W X, 2006. Zero-valent iron nanoparticles for abatement of environmental pollutants: materials and engineering aspects. *Critical Reviews in Solid State and Materials Sciences*, 31(4): 111–122.

Liou Y H, Lo S L, Lin C J, Kuan W H, Weng S C, 2005. Chemical reduction of an unbuffered nitrate solution using catalyzed and uncatalyzed nanoscale iron particles. *Journal of Hazardous Materials*, 127(1-3): 102–110.

Manu B, Chaudhari S, 2003. Decolorization of indigo and azo dyes in semicontinuous reactors with long hydraulic retention time. *Process Biochemistry*, 38(8): 1213–1221.

Masciangioli T, Zhang W X, 2003. Environmental technologies at the nanoscale. *Environmental Science & Technology*, 37(5): 102A–108A.

Muruganandham M, Swaminathan M, 2004. Photochemical oxidation of reactive azo dye with UV-H_2O_2 process. *Dyes and Pigments*, 62(3): 269–275.

Nam S, Tratnyek P G, 2000. Reduction of azo dyes with zerovalent iron. *Water Research*, 34(6): 1837–1845.

Orth W S, Gillham R W, 1996. Dechlorination of trichloroethene in aqueous solution using Fe^0. *Environmental Science & Technology*, 30(1): 66–71.

Ozer R R, Ferry J L, 2001. Investigation of the photocatalytic activity of TiO_2-polyoxometalate systems. *Environmental Science & Technology*, 35(15): 3242–3246.

Pagga U, Brown D, 1986. The degradation of dyestuffs: Part II Behaviour of dyestuffs in aerobic biodegradation tests. *Chemosphere*, 15(4): 479–491.

Park H, Choi W, 2003. Visible light and Fe(III)-mediated degradation of acid Orange 7 in the absence of H_2O_2. *Journal of Photochemistry and Photobiology A: Chemistry*, 159(3): 241–247.

Qu B C, Zhou J T, Xiang X M, Zheng C L, Zhao H X, Zhou X B, 2008. Adsorption behavior of Azo Dye C. I. Acid Red 14 in aqueous solution on surface soils. *Journal of Environmental Sciences*, 20(6): 704–709.

Roberts A L, Totten L A, Arnold W A, Burris D R, Campbell T J, 1996. Reductive elimination of chlorinated ethylenes by zero-valent metals. *Environmental Science & Technology*, 30(8): 2654–2659.

Ruppert G, Bauer R, Heisler G, 1994. UV-O_3, UV-H_2O_2, UV-TiO_2 and the photo-Fenton reaction-comparison of advanced oxidation processes for wastewater treatment. *Chemosphere*, 28(8): 1447–1454.

Saxe J P, Lubenow B L, Chiu P C, Huang C P, Cha D K, 2006. Enhanced biodegradation of azo dyes using an integrated elemental iron-activated sludge system: I. Evaluation of system performance. *Water Environmental Research*, 78(1): 19–25.

Shu H Y, Chang M C, Yu H H, Chen W H, 2007. Reduction of an azo dye Acid Black 24 solution using synthesized nanoscale zerovalent iron particles. *Journal of Colloid and Interface Science*, 314(1): 89–97.

Shu H Y, Huang C R, 1995. Degradation of commercial azo dyes in water using ozonation and UV enhanced ozonation process. *Chemosphere*, 31(8): 3813–3825.

Shu H Y, Huang C R, Chang M C, 1994. Decolorization of mono-azo dyes in wastewater by advanced oxidation process: a case study of acid red 1 and acid yellow 23. *Chemosphere*, 29(12): 2597–2607.

Sohn K, Kang S W, Ahn S, Woo M, Yang S K, 2006. Fe (0) nanoparticles for nitrate reduction: stability, reactivity, and transformation. *Environmental Science & Technology*, 40(17): 5514–5519.

Weber E J, 1996. Iron-mediated reductive transformations: Investigation of reaction mechanism. *Environmental Science & Technology*, 30(2): 716–719.

Zhang C Q, Zhang H F, Lv M Q, Hu Z Q, 2010. Decolorization of azo dye solution by Fe-Mo-Si-B amorphous alloy. *Journal of Non-Crystalline Solids*, 356(33-34): 1703–1706.

Zhang C Q, Zhu Z W, Zhang H F, Hu Z Q, 2011. Rapid reductive degradation of azo dyes by a unique structure of amorphous alloys. *Chinese Science Bulletin*, 56(36): 3988–3992.

Zhao H Z, Sun Y, Xu L N, Ni J R, 2010. Removal of Acid Orange 7 in simulated wastewater using a three-dimensional electrode reactor: Removal mechanisms and dye degradation pathway. *Chemosphere*, 78(1): 46–51.

JOURNAL OF ENVIRONMENTAL SCIENCES